Published in final edited form as:
*Neuron Glia Biol*. 2004 August ; 1(3): 179–192.

# Oligodendrocytes assist in the maintenance of sodium channel clusters independent of the myelin sheath

**JEFFREY L. DUPREE**[1], **JEFFREY L. MASON**[2], **JILL R. MARCUS**[1], **MICHAEL STULL**[3], **ROCK LEVINSON**[4], **GLENN K. MATSUSHIMA**[5,6], and **BRIAN POPKO**[7]

1*Department of Anatomy and Neurobiology Virginia Commonwealth University School of Medicine Richmond, VA 23298*

2*Department of Neurology The Farber Institute Thomas Jefferson University Philadelphia, PA 19107*

3*Department of Pathology and Anatomy Eastern Virginia Medical School Norfolk, VA 23501*

4*Department of Physiology University of Colorado Medical School Denver, Colorado 80262*

5*Department of Microbiology and Immunology University of North Carolina at Chapel Hill Chapel Hill, NC 27599*

6*UNC Neuroscience Center University of North Carolina at Chapel Hill Chapel Hill, NC 27599*

7*Jack Miller Center for Peripheral Neuropathy Department of Neurology University of Chicago Chicago, IL 60637-1470*

## Abstract

To ensure rapid and efficient impulse conduction, myelinated axons establish and maintain specific protein domains. For instance, sodium ($Na^+$) channels accumulate in the node of Ranvier; potassium ($K^+$) channels aggregate in the juxtaparanode and neurexin/caspr/paranodin clusters in the paranode. Our understanding of the mechanisms that control the initial clustering of these proteins is limited and less is known about domain maintenance. Correlative data indicate that myelin formation and/or mature myelin-forming cells mediate formation of all three domains. Here, we test whether myelin is required for maintaining $Na^+$ channel domains in the nodal gap by employing two demyelinating murine models: (1) cuprizone ingestion, which induces complete demyelination through oligodendrocyte toxicity; and (2) ceramide galactosyltransferase deficient mice, which undergo spontaneous adult-onset demyelination without oligodendrocyte death. Our data indicate that the myelin sheath is essential for long-term maintenance of sodium channel domains; however, oligodendrocytes, independent of myelin, provide a partial protective influence on the maintenance of nodal $Na^+$ channel clusters. Thus, we propose that multiple mechanisms regulate the maintenance of nodal protein organization. Finally, we present evidence that following the loss of $Na^+$ channel clusters the chronological progression of expression and reclustering of $Na^+$ channel isoforms during the course of CNS remyelination recapitulates development.

### Keywords

Protein domains; axolemma; node of Ranvier; demyelination

Correspondence should be addressed to: Jeffrey L. Dupree, Ph.D. Anatomy and Neurobiology Sanger Hall 11-073 1101 E. Marshall Street PO Box 980709 Virginia Commonwealth University School of Medicine Richmond, VA 23298 USA; phone: +1 804 828 9536; email: jldupree@vcu.edu.

## INTRODUCTION

The axolemma of myelinated axons is divided into unique molecular domains, the most distinctive of which is the node of Ranvier. Clustered in high density in the nodal gap are voltage-gated $Na^+$ channels, which mediate membrane depolarization resulting in saltatory conduction (Hille and Catterall, 1994). In the paranode, the region flanking each side of the node, myelin maintains its closest apposition to the axon through septate-like junctions. A prominent component of paranodal junctions are transverse bands (TBs), which contain the axolemmal protein known as neurexin/caspr/paranodin (NCP1) (Bhat, 2003). In addition to their role in anchoring the myelin sheath to the axon, TBs form a physical barrier between the nodal $Na^+$ channels and juxtaparanodal $K^+$ channels, which limits lateral migration of these and other axolemmal proteins (Rosenbluth, 1980; Dupree et al., 1999; Bhat et al., 2001; Boyle et al., 2001; Rios et al., 2003).

Normally, paranodal junctions maintain ion-channel domains, but they are not required for initial clustering of $Na^+$ channels at the node (Dupree et al., 1999; Rasband et al., 2003a). The mechanisms that regulate the initial organization of these protein domains are not fully understood. Because protein domain clustering coincides with myelination, it has been postulated that formation of a compact myelin sheath regulates protein distribution in mature, myelinated nerve fibers (Dugandzija-Novakovic et al., 1995; Baba et al., 1999). Recently, Rios et al. (Rios et al., 2003) refined this idea by demonstrating that formation of nodal/paranodal protein domains is regulated by paranodal interactions that are independent of the internodal compact myelin sheath. Although they distinguished between the roles of the paranode and compact myelin, these findings still indicate the need for physical contact between the axon and the myelinating cell (Rios et al., 2003). In contrast to the physical contact theory, Kaplan et al. (Kaplan et al., 1997) demonstrated that clustering of $Na^+$ channels is not dependent on myelin formation and paranodal cell—cell interactions. They proposed that a soluble factor released by oligodendrocytes initiates channel clustering. Furthermore, Deerinck et al. (Deerinck et al., 1997) provided convincing evidence that contact between the myelin-forming cell and the axon is not required for $Na^+$ channel clustering. Thus, two, not necessarily exclusive, theories explaining nodal domain formation persist. Additionally, two groups showed that the immature $Na^+$ channel isoform 1.2 ($Na_v$ 1.2) concentrates at newly formed nodes before clustering of the mature isoform $Na_v$ 1.6 (Boiko et al., 2001; Kaplan et al., 2001). Little is known regarding the regulation of the expression and distribution of specific isoforms; however, physical contact at the paranode appears to be involved (Rios et al., 2003).

## OBJECTIVE

In this study we determine whether the maintenance of $Na^+$ channel clustering requires myelin contact or if the presence of oligodendrocytes is sufficient. We achieve this by comparing nodal clustering of ion channels in the presence and absence of oligodendrocytes in two *in vivo* models of demyelination. By exploiting these models, we present compelling evidence that, in the absence of myelin, oligodendrocytes protect against the rapid loss of nodal $Na^+$ channel clustering, and that this effect is independent of myelin—axon contact.

## METHODS

### Models

Mice deficient in ceramide galactosyltransferase (CGT) form abundant CNS myelin that undergoes dramatic, spontaneous degeneration (Coetzee et al., 1996). Although demyelination is extensive, oligodendrocytes are spared, even in regions of extensive demyelination, and they express normal levels of myelin-specific genes even at the terminal life expectancy of these

mutants (Coetzee et al., 1998). Demyelination in CGT-deficient mice is not accompanied by CNS infiltration of T cells, but microglial activation and astrogliosis are prevalent (Coetzee et al., 1998). By contrast, cuprizone (biscyclohexanone oxaldihydrazone)-induced demyelination is initiated by cellular toxicity that is specific to oligodendrocytes when administered at the concentrations used in this study (Matsushima and Morell, 2001). Similar to the demyelination in CGT deficient mice, cuprizone does not induce a T-cell-mediated inflammatory response; however, microglia and astrocyte activation is observed (McMahon et al., 2001).

CGT-deficient and the cuprizone-treated models were chosen because they provide the opportunity to compare the maintenance of $Na^+$ channel clustering following demyelination in either the presence or absence of oligodendrocytes. Although there are several models of demyelination induced by oligodendrocyte death (Gilson and Blakemore, 2002; Tompkins et al., 2002; Bieber et al., 2003), cuprizone requires no surgical procedures and physical trauma. Furthermore, the cuprizone model is well characterized and provides a highly reproducible lesion with regard to the onset, extent and CNS location of demyelination (Hiremath et al., 1998; Mason et al., 2000; Mason et al., 2001; McMahon et al., 2001). The CGT model was chosen because we (Coetzee et al., 1998) and others (Bosio et al., 1998) have extensively characterized the demyelinating events in these mice, and it is the only murine model that provides reproducible, adult-onset CNS demyelination without oligodendrocyte death.

For this study CGT-deficient and wild-type (WT) litter-mates were weaned at post-natal day (PND) 28 and maintained on a diet of ground feed and Transgel™ (Harlan Sprague-Dawley). The mice were monitored closely and sub-cutaneous injections of sterile saline were given as needed to prevent dehydration. Mice were sacrificed between PND 15 and 101 (a rare age for the CGT-mutant mice because of the severity of the phenotype) (Dupree et al., 1998a). For the cuprizone studies, 8-week-old C57Bl6 male mice were fed ground feed containing 0.2% cuprizone (w/w) for 2, 3, 4, 5 and 6 weeks. Animals maintained on this diet exhibit minimal toxic effects, other than regional CNS demyelination, which is observed at both the gross and microscopic levels (Mason et al., 2000; Mason et al., 2001). As stated previously, the toxic effects are specific to oligodendrocytes at this dose (Matsushima and Morell, 2001). A further group of mice were fed cuprizone-containing feed for 6 weeks and then maintained for an additional 2 weeks on normal feed to maximize remyelination.

## Electron microscopy

To determine the time course and extent of demyelination in the spinal cord and optic nerve of CGT-mutant mice and in the corpus callosum of the cuprizone-treated mice, whole body, transcardial perfusions were performed using a phosphate buffered solution containing 4% paraformaldehyde and 2.5% glutaraldehyde (pH 7.3). The mice were post-fixed in the same solution for 2 weeks and appropriate tissues harvested and processed for standard transmission electron microscopic analysis as described previously (Dupree et al., 1998b; Mason et al., 2001). A minimum of eight images per animal were collected at 15 000× magnification using a JEOL 1200 transmission electron microscope to quantify the extent and time course of demyelination. For the CGT mice, images were collected from the ventral columns of the cervical spinal cord and the optic nerve. For the cuprizone-treated mice, images were collected from the corpus callosum at the level of the fornix. These specific CNS regions were chosen because they display the greatest degree of demyelination and are the best characterized. For the quantitative study, an axon was categorized as ‘myelinated’ if it displayed a complete, single wrap of an oligodendrocyte process. Additionally, higher-magnification electron micrographs were collected to analyze and document the cellular contact that was maintained in the demyelinated regions of both the CGT-mutant and cuprizone-treated mice. For this analysis, an oligodendrocyte process was identified by dense cytoplasm and the absence of intermediate filaments. By contrast, astrocytic processes were identified by the presence of

bundled intermediate filaments that are highly characteristic of glial fibrillary acidic protein (GFAP) and glycogen.

### Immunocytochemistry

Transcardial, whole-body perfusions with phosphate buffer (PB; pH 7.3) containing 4% paraformaldehyde were performed at PND 15, 30, 60, 90 and 101 in CGT-mutant mice; cuprizone-treated mice were perfused following either 2, 3, 4, 5 and 6 weeks of treatment or 6 weeks of treatment with an additional 2 weeks of normal feed to maximize remyelination. Transcardial whole body perfusions with phosphate buffer (PB; pH 7.3) containing 4% paraformaldehyde were performed on the mice at the appropriate time points. For the CGT mutants, mice were perfused at PND 15, 30, 60, 90 and 101; for the cuprizone-treated mice, perfusions were performed according to the schedule outlined above. Tissue was harvested, post-fixed for 20 minutes in the same fixative and cryoprotected in PB containing 30% sucrose at 4°C. Tissue samples were oriented appropriately and frozen in Tissue-Tek O.C.T. Embedding Compound (Sakura Finetek USA, Inc.). Consecutive, 10 μm, longitudinal, frozen sections of the optic nerve and ventral column of the spinal cord from CGT mice, and coronal, frozen sections of the corpus callosum at the level of the fornix from cuprizone-treated mice were double-labeled as described previously (Dupree et al., 1999) with antibodies directed against (1) a highly conserved region of $Na^+$ channels (mouse monoclonal, dilution 1:100, clone K58/35; Sigma) and NCP1 (rabbit polyclonal, dilution 1:1000; kindly provided by Dr Elior Peles), (2) $Na^+$ channel isoform type $Na_v$ 1.6 (rabbit polyclonal, dilution 1:100; Boiko et al., 2003) and $K^+$ channel Kv1.1 (mouse monoclonal, dilution 1:100; Upstate Biotechnology), (3) pan-$Na^+$ channel (clone K58/35) and myelin basic protein (MBP) (rabbit polyclonal, dilution 1:200; Dako-Cytomation Inc.), and (4) pan-$Na^+$ channel (clone K58/35) and myelin associated glycoprotein (MAG) (rat polyclonal, 1:10; R&D Systems). Frozen sections were single immunolabeled with an antibody directed against $Na^+$ channel isoform type $Na_v$ 1.2 (rabbit polyclonal; Upstate Biotechnology). Additionally, the cc-1 antibody (mouse monoclonal, dilution 1:20; EMD Biosciences) (Bhat et al., 1996) was used to determine oligodendrocyte number in the optic nerve and spinal cord of CGT-deficient mice and the corpus callosum in cuprizone-treated animals. The cc-1 antibody was also used in tandem with the pan-$Na^+$ channel antibody (clone K58/35). Although both antibodies are of mouse origin, distinct morphologies and distributions allow this application, and similar approaches have been employed successfully (Traka et al., 2002). Following thorough rinsing of the primary antibodies, sections were incubated in the appropriate secondary antibodies conjugated with either FITC or Texas red (Vector Laboratories Inc.).

### Quantitation of $Na^+$ channel clusters and oligodendrocytes

Using a combination of immunocytochemistry and confocal microscopy, the numbers of oligodendrocytes and $Na^+$ channel clusters were determined. For each animal, a minimum of six microscopic z-fields were collected for quantitation. For this work, a z-field is defined as a maximum projection image produced by collecting and compiling 16 optical sections, each 0.4 μm apart. Thus, each maximum projection image is a two-dimensional representation of a three-dimensional image that is 6.0 μm high. All images were collected with a pinhole of 0.5 Airy disc units for increased resolution using a Zeiss 510 laser scanning confocal microscope (Carl Zeiss Microimaging) equipped with a krypton/argon laser (excitation 488 nm) and a helium/neon laser (excitation 543 nm).

### Western blot

Western blots were used to analyze the change in $Na^+$ channel expression in mice maintained on a cuprizone-containing diet. For these studies, the corpus callosum was isolated from cuprizone-treated mice and homogenized in 1% SDS in PB. Protein samples (20 μg) were

loaded and separated on a 10% Bis-Tris NuPage™ (Invitrogen Inc.) gel. After transfer onto nitrocellulose, blots were incubated with clone K58/3, monoclonal pan-$Na^+$ channel antibody (dilution 1:1000). The bands were visualized using ECL-plus Chemiluminescence (Amersham Biosciences).

## RESULTS

### In the absence of oligodendrocyte death (CGT-mutant mice)

**Demyelination—**Because the primary focus of this study was to analyze the maintenance of $Na^+$ channel clusters in the absence of myelin, we employed transmission electron microscopic techniques to quantify the extent of demyelination in the spinal cord and optic nerve of CGT mutants. As previously reported, little or no evidence of demyelination, such as myelin vacuolation, myelin debris and microglial activation, was observed in the CNS at PND 30 (Dupree et al., 1998c). However, significantly more axons in the CNS of mutant mice were unmyelinated at this time point (Fig. 1A), which confirms our previous findings (Marcus et al., 2000). By ~2 months of age both the spinal cord and optic nerve contained many unmyelinated axons with nearly 2/3 of axons completely bare of myelin and oligodendrocytic processes. This increase in unmyelinated axons was accompanied by myelin debris, vacuolated myelin sheaths and activated microglia (not shown). By PND 90, 60% of the axons in the cervical spinal cord lacked oligodendrocyte ensheathment (Fig. 2C,D), determined by either a myelin sheath or a single, complete oligodendrocytic wrap. For the axons that displayed some degree of oligodendrocyte ensheathment (nearly 40%), approximately half of the sheaths were extremely thin, which is indicative of remyelination. By contrast, by PND 90 the optic nerve was nearly devoid of myelin (Fig. 1D; Fig. 2A,B).

Although demyelination was a prevalent finding in the CNS of aged, CGT-mutant mice, frequently the unmyelinated axons maintained glial contact. As shown in Fig. 3, these unmyelinated axons were ensheathed by astrocytic processes, which were identified by the presence of glycogen and tightly bundled intermediate filaments characteristic of GFAP (Fig. 3). Our electron microscopical analysis confirms our earlier report that upregulation of GFAP mRNA and protein accompanies demyelination in CGT-deficient mice (Coetzee et al., 1998). Although far less frequent, some axons were seen to be ensheathed by an oligodendrocytic process; such axons were counted as ‘myelinated’. Additionally, we occasionally observed oligodendrocytic processes coursing between and, thus, contacting unmyelinated axons.

**Oligodendrocyte survival—**Using *in situ* hybridization, we have shown previously that the number of oligodendrocytes is the same in CGT-mutant mice and littermate, WT animals at PND 5 and 30 (Marcus et al., 2000). Furthermore, Northern blot data indicate no change in the number of oligodendrocytes at PND 90 (Coetzee et al., 1998). Because the absence of oligodendrocyte death is key for the present work, we employed a third method to demonstrate that oligodendrocyte death is not a prominent event in the CGT mutants. By immunolabeling frozen sections of spinal cord and optic nerve at PND 15, 30 and 90 with antibodies directed against the oligodendrocyte cell body marker cc-1, we provide compelling evidence that there is no change in the number of CNS myelin-forming cells throughout the life of these animals (Fig. 1C; Fig. 4A,B). Furthermore, our current immunocytochemical findings correlate well with our previous work showing that the number of oligodendrocytes in CGT-mutant mice is ~50% higher than in age-matched, WT animals (Marcus et al., 2000). This sustained survival of the oligodendrocyte population, even at the terminal life expectancy of these mice, indicates that wholesale oligodendrocyte death does not occur in adult, CGT-mutant animals.

**Reduced $Na^+$ channel clusters in aged CGT mutants—**We reported previously that NCP1 and $K^+$ channels do not localize normally in the spinal cord of CGT-deficient mice (Dupree et al., 1999). By contrast, $Na^+$ channels cluster in nodal regions in the spinal cord of

these mutant animals (Dupree et al., 1999; Marcus et al., 2002; Rosenbluth et al., 2003; Rasband et al., 2003a). Here, we have determined the number of $Na^+$ channel clusters in axo—glial mutants before and after demyelination. At PNDs 15 and 30 (Fig. 1E), there are no statistical difference in the number of clusters in either the optic nerve (Fig. 5A,B) or spinal cord (Fig. 6A,B), although our counts indicate a slight reduction in cluster number. Similarly, a reduction in $Na^+$ channel clusters has been reported previously in the CNS of these mice (Rasband et al., 2003a). By 2 months of age, the number of $Na^+$ channel clusters in the optic nerve remained constant even though nearly twice as many optic nerve axons lacked myelin compared with PNDs 15 and 30. Thus, dramatic demyelination was not accompanied by a rapid loss of $Na^+$ channel clusters. To maximize the extent of demyelination, and thus the effect of myelin loss, we also determined the number of clusters in the optic nerve and spinal cord at PND 90, an age that fewer than 5% of these mice achieve (Dupree et al., 1998a). By PND 90 the number of $Na^+$ channel clusters was significantly less in the mutant mice compared with age-matched, WT mice (Fig. 1). To accurately evaluate the maintenance of $Na^+$ channel clusters in these animals, we compared the number of clusters observed in mutant animals at PND 30 and 60 with those at PND 90. Importantly, our counts indicate that only 46% of the clusters in the optic nerve and 30% of the clusters in the spinal cord are lost during the course of extensive demyelination; the clusters that remained lacked clearly defined borders and frequently appeared elongated, perhaps signifying domain instability (Fig. 5D; Fig. 6C). Although the number of clusters is reduced significantly, a substantial number of clusters remain at PND 101 (Fig. 6D), more than 8 weeks after the onset of extensive demyelination (Fig. 1A) (Coetzee et al., 1996). Furthermore, the findings with the pan-$Na^+$ channel antibody (clone K58/35) are corroborated by the qualitative analysis of $Na_v$ 1.6 (not shown), which indicates that the number of $Na^+$ channel clusters is not maintained by the formation of new nodes containing the immature isoform $Na_v$ 1.2.

To analyze more directly the relationship between myelin and $Na^+$ channel clusters, we used double-label immunocytochemistry on CGT-deficient and WT optic nerve and spinal cord at PND 90. Although slightly more intense in the spinal cord than in the optic nerve, both myelin markers (antibodies directed against MBP and MAG) revealed minimal labeling of myelin, which further indicates the extensive demyelination that occurs in these mice. Furthermore, $Na^+$ channel clusters were distributed uniformly with no apparent preference for myelinated regions (data not shown). $Na^+$ channel clusters were visualized easily in areas that contained myelin and in those that lacked myelin. Additionally, we used similar techniques to determine if the $Na^+$ channel clusters are better maintained in regions that contain many oligodendrocytes. In the spinal cord and optic nerve, both oligodendrocytes and $Na^+$ channel clusters were distributed evenly, thus, it is not clear if oligodendrocyte distribution influences $Na^+$ channel clusters locally.

**Re-expression of $Na_v$ 1.2—**Our electron microscopic study (Fig. 2) indicated CNS remyelination in CGT-mutant mice, so we analyzed the expression of the immature $Na^+$ channel isoform. Minimal expression of $Na_v$ 1.2 was observed in the optic nerve and the spinal cord from CGT-mutant mice and their WT litter-mates at PND 30. By PND 90 immunoreactivity in both the optic nerve and the spinal cord of mutant mice increased dramatically. A few $Na_v$ 1.2 clusters, presumably nodal, were observed in the spinal cord. However, numerous, small, focal concentrations, less than 1 μm long, were abundant and accompanied by extended regions of diffuse labeling. These small concentrations and the diffuse labeling appeared in a linear orientation as though they were aligned along an axon. Based on cluster size, presumed nodal clusters were not observed in the optic nerve. However, small concentrations and diffuse labeling, similar to that described in the spinal cord were abundant and oriented similarly (data not shown).

## Demyelination in response to oligodendrocyte death (cuprizone-treated mice)

**Demyelination—**Using light and electron microscopic techniques, we have shown previously that cuprizone-treatment results in complete demyelination of the corpus callosum (Hiremath et al., 1998; Mason et al., 2001). Here, we confirm the extent of demyelination in the corpus callosum of cuprizone-exposed mice through electron microscopic analyses (Fig. 7). As previously shown, there is no increase in the number of unmyelinated axons in the corpus callosum following 3 weeks of cuprizone treatment (Fig. 8A). After 4 weeks of treatment, ~85% of axons lacked myelin (Fig. 7B; Fig. 8A) and nearly complete demyelination of the corpus callosum occurred following 5 weeks of treatment (Fig. 7C). Substantial remyelination was evident after 6 weeks of continuous cuprizone treatment (Fig. 7D; Fig. 8A), which is consistent with our previous reports (Mason et al., 2001). Although not shown, removal of cuprizone from the diet resulted in continued, robust remyelination.

**Oligodendrocyte survival—**Our previous characterization of the cuprizone model demonstrated that a low dose of this toxin begins to deplete the oligodendrocyte population in the corpus callosum after 2 weeks of exposure (Mason et al., 2000). Immunoreactivity against the cc-1-oligodendrocyte cell body marker (Bhat et al., 1996; Armstrong et al., 2002) revealed robust labeling in the corpus callosum of untreated mice (Fig. 8C; Fig. 9A). By contrast, we observed almost no oligodendrocytes in the corpus callosum of mice treated with cuprizone for 2-4 weeks (Fig. 8C; Fig. 9B). By 5 weeks of treatment a few cc-1-positive cells were observed (Fig. 8C; Fig. 9C), and after 6 weeks exposure, there was substantial repopulation of the corpus callosum by presumably newly formed oligodendrocytes (Fig. 8C; Fig. 9D). It is important to note that the loss of oligodendrocytes precedes the initiation of demyelination by ~2 weeks.

**Complete disruption of $Na^+$ channel clustering—**We next analyzed maintenance of $Na^+$ channel clusters in the absence of both myelin and oligodendrocytes using the cuprizone-treated mice. In the mice maintained on normal feed, immunoreactivity for the pan-$Na^+$ channel antibody (Fig. 10A) and the $Na_v$ 1.6 antibody (data not shown) was robust. Following 3 weeks of cuprizone treatment, <50% (13 out of 29) of the original $Na^+$ channel clusters remained in the corpus callosum (Fig. 8B; Fig. 10C). Interestingly, little structural change was observed in the myelin sheaths, but widespread oligodendrocyte death was evident. Loss of $Na^+$ channel clustering progressed through 5 weeks of treatment, at which time little or no clustering was observed (Fig. 8B; Fig. 10E). After 6 weeks treatment, $Na^+$ channel clusters were observed again. Although $Na^+$ channel clustering reduced dramatically between 2-6 weeks, Western blot analysis revealed no change in $Na^+$ channel expression during this time (data not shown).

**NCP1 and $K^+$ channel clustering—**Similar to $Na^+$ channels, clustering of both NCP1 (Fig. 10C) and $K^+$ channels (data not shown) was reduced initially following 3 weeks of treatment and the loss of clustering of these axolemmal proteins coincided with continued demyelination. Following 6 weeks treatment, a few NCP1 clusters reappeared and these paranodal accumulations frequently bracketed clustered $Na^+$ channels.

**$Na^+$ channel reclustering—**An increase in $Na^+$ channel clustering was observed following 6 weeks of treatment compared with 4 and 5 weeks of cuprizone exposure (Fig. 8; Fig. 10). Such increased immunoreactivity patterns indicate nodal reclustering of $Na^+$ channels. Developmental studies report that $Na_v$ 1.2 is expressed transiently in immature nodes of Ranvier, so we determined which isoform is expressed in the reforming nodes during remyelination. Following 2 weeks of treatment, before the loss of $Na^+$ channel clustering, the expression of $Na_v$ 1.2 was minimal (Fig. 11A). Following 6 weeks of treatment, the immunoreactivity of the $Na_v$ 1.2 antibody increased and the labeling pattern revealed some clusters that were consistent in size, shape and intensity with nodal clusters (Fig. 11B). Similar

to the pattern of $Na_v$ 1.2 labeling observed in CGT mice, numerous small concentrations (<1 μm long) that were frequently distributed in linear arrays, were observed in the corpus callosum of cuprizone-treated mice (Fig. 11B). $Na_v$ 1.2 expression was transient because mice that were maintained for an additional 2 weeks on a non-cuprizone diet following 6 weeks of cuprizone exposure displayed minimal $Na_v$ 1.2 clustering (Fig. 11C). Following 6 weeks of cuprizone exposure, $Na_v$ 1.6 reclustering was observed, but whether newly formed nodes expressed both $Na_v$ 1.2 and $Na_v$ 1.6 is not known.

## CONCLUSIONS

- CGT-mutant mice undergo extensive CNS demyelination in the absence of oligodendrocyte death and a slight, but highly reproducible, reduction in the number of CNS $Na^+$ channel clusters.
- When demyelination is nearly complete, $Na^+$ channel clusters are partially preserved only in the presence of viable oligodendrocytes.
- $Na^+$ channel clusters reform during remyelination, and new clusters contain the immature $Na^+$ channel isoform, $Na_v$ 1.2.
- $Na_v$ 1.2 is observed first in numerous small clusters (<1 μm), which are distributed in a linear array. With time, the small clusters are replaced by fewer, larger clusters (>1 μm).

## DISCUSSION

In this study we present evidence that oligodendrocytes, independent of myelin, provide a partial protective influence against the loss of nodal $Na^+$ channel clusters. Our findings indicate that, following demyelination, the loss of $Na^+$ channel clusters is delayed by the presence of viable oligodendrocytes. However, oligodendrocytes alone (i.e. in the absence of a myelin sheath) are not sufficient for long-term maintenance of normal $Na^+$ channel domains, which indicates that axolemmal protein domains are maintained by multiple mechanisms. Additionally, we present evidence that remyelination-induced reclustering of CNS $Na^+$ channel domains in adults recapitulates development. During remyelination, the immature $Na^+$ channel isoform $Na_v$ 1.2 is expressed transiently in presumptive immature nodal clusters in the CNS and precedes that of $Na_v$ 1.6. This expression sequence is similar to that which occurs during development (Boiko et al., 2001; Kaplan et al., 2001). Our data also indicate that small accumulations of $Na_v$ 1.2 form along the axon following demyelination, coincident with remyelination, and that these small, non-nodal concentrations coalesce to form immature nodal clusters.

### Galactolipid-deficient versus cuprizone-induced demyelinating models

The basic premise of this work is that oligodendrocytes, independent of a myelin sheath, provide a partial protective effect on nodal $Na^+$ channel clusters following demyelination. To test this hypothesis we employed two murine models of demyelination in which CNS demyelination is accompanied by microglial and astroglial activation without T-cell inflammation (Coetzee et al., 1998; McMahon et al., 2001). However, these models differ in the regions of the CNS that are most susceptible to myelin loss and in the fate of the oligodendrocytes. Here, and in previous studies (Mason et al., 2000), we demonstrate that oligodendrocytes in the corpus callosum of cuprizone-treated mice die within 2-3 weeks of exposure. In contrast, oligodendrocyte cell death is not observed in adult CGT-deficient mice (Coetzee et al., 1998) and these mice maintain an enhanced population of myelin-forming cells (Marcus et al., 2000). In this regard, CGT-deficient mice provide a unique model of demyelination because oligodendrocytes do not die.

### Initial $Na^+$ channel cluster formation

Several studies have indicated that the initial clustering of $Na^+$ channels in the CNS is regulated by axon—oligodendrocyte interactions, but the precise mechanism of nodal clustering remains elusive. Recently, Rios et al. utilized the NCP1-null mouse, which forms relatively normal compact myelin but has abnormal paranodal structure, to demonstrate that paranodal interactions, independent of compact internodal myelin, regulate the expression and distribution of $Na^+$ channels (Rios et al., 2003). Similarly, CGT-mutant mice maintain abundant, nodal, $Na^+$ channel clusters (Marcus et al., 2002; Rosenbluth et al., 2003). These are slightly elongated (Dupree et al., 1999; Rasband et al., 2003a), presumably as a result of the abnormal paranodal interactions that are prominent in these animals (Dupree et al., 1998a). Interestingly, the overall nodal and paranodal ultrastructure is normal in the CNS of CGT-deficient mice at PND 15, when the proteins that aggregate in these domains are actively clustering (Marcus et al., 2002; Boiko et al., 2003). With normal paranodal structure, normal clustering is to be expected. Here, we report a slight reduction in the number of $Na^+$ channel clusters in both the optic nerve and the spinal cord at PNDs 15 and 30 (Fig. 1). Our findings are supported by Rasband et al., who also report that the number of $Na^+$ channel clusters is reduced in adolescent and young adult CGT-mutant mice (PND 15-35) without a reduction in $Na^+$ channel expression (Rasband et al., 2003a). One explanation for the decrease in $Na^+$ channel clusters might be that an increase in internodal length effectively reduces the number of nodes that are formed. Alternatively, we propose that it results from a significant increase in the number of axonal segments that are never myelinated, possibly as a function of the limited capacity of these mice to produce normal levels of myelin membrane (Marcus et al., 2000). In support of this hypothesis, mice that lack sulfatide (CST-deficient) (Honke et al., 2002), have no significant increase in unmyelinated axons (Marcus and Dupree, unpublished observations) but initially form normal numbers of $Na^+$ channel nodal clusters (Ishibashi et al., 2002).

### Maintenance of axolemmal protein domains

Although nodal $Na^+$ channel clusters are abundant in the CNS of CGT-deficient mice, the borders of the ion channel domains become less defined with increasing age. Similarly, as CST-deficient mice age, the $Na^+$ channel clusters elongate and eventually disappear (Ishibashi et al., 2002). In both CGT and CST-deficient mice, the elongation and ultimate loss of the channel domains requires many weeks. Because both mutants display abnormal paranodal structure (Dupree et al., 1998b; Honke et al., 2002), it is possible that the progressive disorganization of the paranode is responsible for the gradual loss of $Na^+$ channel clusters. We predict that, even in the presence of oligodendrocytes, $Na^+$ channel clusters would eventually disappear in the CNS of the CGT mutants if these animals survived significantly longer. Thus, we propose that the protective influence that oligodendrocytes provide against cluster loss is only partial. In support of our hypothesis, Ellisman and Levinson used freeze fracture and immunocytochemical analyses to postulate that the mechanisms that preserve membrane domains within the axolemma are independent of myelination (Ellisman, 1979; Ellisman and Levinson, 1982). Additionally, Arroyo et al. (Arroyo et al., 2002) report that $Na^+$ channel clusters persist in the CNS of *myelin deficient* (*md*) rats after myelin and oligodendrocytic ensheathments are lost. Although the loss of myelin and myelin ensheathments results from oligodendrocyte death in *md* rats, some oligodendrocytes survive. Thus, persistence of $Na^+$ channel clusters might also result from a protective effect of the remaining oligodendrocytes. An alternative explanation for the persistence of $Na^+$ channel clusters in *md* rats is that the myelin-bare axons had only recently demyelinated and lateral migration of the ion channels was in progress but not complete at the time of death. The time required for $Na^+$ channels to uncluster following demyelination is not known fully. Here, using the cuprizone system, we demonstrate that $Na^+$ channel clusters are lost completely within 1 week of demyelination. Similarly, Dugandzija-Novakovic et al. reported that $Na^+$ channel clusters remain stable for ~1 week following demyelination (Dugandzija-Novakovic et al., 1995). By contrast, the CGT

mice continue to maintain a large number of $Na^+$ channel clusters for at least 8 weeks after the onset of CNS demyelination. Moreover, at ~2 months of age, the number of unmyelinated fibers in the optic nerve is double that at 1 month of age, but the number of $Na^+$ channel clusters does not change. Thus, CGT-deficient mice preserve significant numbers of $Na^+$ channel clusters longer than other demyelinating models. The major difference between the CGT mutants and other demyelinating systems is sparing of the myelin-forming cells. Thus, our findings indicate that oligodendrocytes, independent of myelin, partially preserve nodal clustering of $Na^+$ channels.

With regard to the cuprizone model, it is important to note that the first significant loss of $Na^+$ channel clusters occurs after 3 weeks of treatment. This loss occurs before demyelination and appreciable structural changes in the myelin sheath, but corresponds precisely with the loss of oligodendrocytes. By 4 weeks of treatment, only 20% of the $Na^+$ channel clusters remain intact, which indicates that the loss of oligodendrocytes results in $Na^+$ channel unclustering. Similarly, using temporally controlled oligodendrocyte ablation, Mathis et al. concluded that formation and maintenance of axolemmal protein domains requires these myelin-forming cells (Mathis et al., 2001). By contrast, Kaplan et al. (Kaplan et al., 1997) reported that removal of oligodendrocytes from neuronal cultures did not result in a loss of $Na^+$ channel clustering. One important distinction between the *in vitro* system used previously (Kaplan et al., 1997; Kaplan et al., 2001) and the *in vivo* model used in the present study is that only $Na_v$ 1.2 clusters in the *in vitro* system. Thus, the difference in maintenance of $Na^+$ channel clusters observed in these studies might reflect different requirements for maintenance of the distinct $Na^+$ channel isoforms.

Another cell type that might be involved in establishing and maintaining nodal $Na^+$ channel clusters in the CNS is the astrocyte. Astrocytes extend processes that ensheath the node of Ranvier and are, thus, fortuitously positioned to assist in the formation and maintenance of nodal axolemmal organization. In both CGT-deficient and cuprizone-treated mice, demyelination is accompanied by a dramatic upregulation of GFAP and astrocytic process formation. From our electron microscopic analysis, myelin-bare axons in both models are associated closely with astrocytic extensions. Although we can not completely rule out a role for astrocytes in maintaining $Na^+$ channel clusters, it appears that both demyelinating models should be equally influenced by astrocytes because astrogliosis is prevalent and consistent in both.

## Molecular re-organization of CNS axons recapitulates development

Initiation of $Na^+$ channel cluster formation is not restricted to development but also occurs during remyelination (Craner et al., 2003). During development, immature CNS nodes of Ranvier transiently express $Na_v$ 1.2, which is replaced by $Na_v$ 1.6 as the animals age (Kaplan et al., 2001; Boiko et al., 2001). Although this sequence of isoform expression has been documented during development, we provide conclusive evidence that $Na_v$ 1.2 is re-expressed following demyelination. In both demyelinating models used, immunoreactivity for $Na_v$ 1.2 increases dramatically. In the optic nerve, where remyelination was not observed, $Na_v$ 1.2 immunoreactivity appears as both diffuse labeling and focal accumulations that are much smaller than nodal clusters, along extended regions of the axon. By contrast, nodal clusters of $Na_v$ 1.2 are prominent in the spinal cord, where indications of remyelination are prevalent. Thus, formation of clusters that are consistent in size with nodal clusters coincides temporally with remyelination. Our findings are supported by previous studies that report upregulation of $Na_v$ 1.2 following demyelination (Rasband et al., 2003b) and remyelination (Craner et al., 2003) of the optic nerve. These findings are particularly important because $Na_v$ 1.2 and $Na_v$ 1.6 have different electrophysiological properties (Smith et al., 1998), which might result in different impulse-propagation efficiencies of myelinated axons. Thus, a more complete

understanding of the neuronal and glial factors that regulate the expression and distribution of $Na^+$ channel isoforms might provide insight for novel treatments of human demyelinating disease.

## ACKNOWLEDGEMENTS

We wish to thank Dr Elior Peles for his generous gift of the NCP1 antibody and Stefany Honigbaum for formatting figures, preparing graphs and editorial assistance. The authors acknowledge the helpful contribution of discussions with colleagues at the Myelin Repair Foundation. This work was supported by grants from the NMSS (PP 0770/T, J.D.), the Wadsworth Foundation (Young Investigator Award, J.D.), the NIH (NS27336, B.P.), and a transition award grant from the NMSS (TA 3004A2/T, J.L.M.).

## REFERENCES

Armstrong RG, Le TQ, Frost EE, Borke RC, Vana AC. Absence of fibroblast growth factor 2 promotes oligodendroglial repopulation of demyelinated white matter. Journal of Neuroscience 2002;22:8574–8585. [PubMed: 12351731]

Arroyo EJ, Xu T, Grinspan J, Lambert S, Levinson SR, Brophy PJ, et al. Genetic dysmyelination alters the molecular architecture of the nodal region. Journal of Neuroscience 2002;22:1726–1737. [PubMed: 11880502]

Baba H, Akita H, Ishibashi T, Inoue Y, Nakahira K, Ikenaka K. Completion of myelin compaction, but not the attachment of oligodendroglial processes triggers K(+) channel clustering. Journal of Neuroscience Research 1999;58:752–764. [PubMed: 10583907]

Bieber AJ, Kerr S, Rodriguez M. Efficient central nervous system remyelination requires T cells. Annals of Neurology 2003;53:680–684. [PubMed: 12731006]

Bhat MA, Rios JC, Lu Y, Garcia-Fresco GP, Ching W, St Martin M, et al. Axon—glia interactions and the domain organization of myelinated axons requires neurexin IV/Caspr/Paranodin. Neuron 2001;30:369–383. [PubMed: 11395000]

Bhat MA. Molecular organization of axo—glial junctions. Current Opinions in Neurobiology 2003;13:552–559.

Bhat RV, Axt KJ, Fosnaugh JS, Smith KJ, Johnson KA, Hill DE, et al. Expression of the APC tumor suppressor protein in oligodendroglia. Glia 1996;17:169–174. [PubMed: 8776583]

Boiko T, Van Wart A, Caldwell JH, Levinson SR, Trimmer JS, Matthews G. Functional specialization of the axon initial segment by isoform-specific sodium channel targeting. Journal of Neuroscience 2003;23:2306–2313. [PubMed: 12657689]

Boiko T, Rasband MN, Levinson R, Caldwell JH, Mandel G, Trimmer JS, et al. Compact myelin dictates the differential targeting of two sodium channel isoforms in the same axon. Neuron 2001;30:91–104. [PubMed: 11343647]

Bosio A, Bussow H, Adam J, Stoffel W. Galactosphingolipids and axono—glial interaction in myelin of the central nervous system. Cell and Tissue Research 1998;292:199–210. [PubMed: 9560463]

Boyle ME, Berglund EO, Murai KK, Weber L, Peles E, Ranscht B. Contactin orchestrates assembly of the septate-like junctions at the paranode in myelinated peripheral nerve. Neuron 2001;30:385–397. [PubMed: 11395001]

Coetzee T, Dupree JL, Popko B. Demyelination and altered expression of myelin-associated glycoprotein isoforms in the central nervous system of galactolipid-deficient mice. Journal Neuroscience Research 1998;54:613–622.

Coetzee T, Fujita N, Dupree J, Shi R, Blight A, Suzuki K, et al. Myelination in the absence of galactocerebroside and sulfatide: normal structure with abnormal function and regional instability. Cell 1996;86:209–219. [PubMed: 8706126]

Craner MJ, Lo AC, Black JA, Waxman SG. Abnormal sodium channel distribution in optic nerve axons in a model of inflammatory demyelination. Brain 2003;126:1552–1561. [PubMed: 12805113]

Deerinck TJ, Levinson SR, Bennett GV, Ellisman MH. Clustering of voltage-sensitive sodium channels on axons is independent of direct Schwann cell contact in the dystrophic mouse. Journal of Neuroscience 1997;17:5080–5088. [PubMed: 9185545]

Dugandzija-Novakovic S, Koszowski AG, Levinson SR, Shrager P. Clustering of $Na^+$ channels and node of Ranvier formation in remyelinating axons. Journal of Neuroscience 1995;15:492–503. [PubMed: 7823157]

Dupree JL, Suzuki K, Popko B. Galactolipid in the formation and function of the myelin sheath. Microscopy Research and Technique 1998a;41:431–440. [PubMed: 9672425]

Dupree JL, Coetzee T, Blight A, Suzuki K, Popko B. Myelin galactolipids are essential for proper node of Ranvier formation in the CNS. Journal of Neuroscience 1998b;18:1642–1649. [PubMed: 9464989]

Dupree JL, Coetzee T, Suzuki K, Popko B. Myelin abnormalities in mice deficient in galactocerebroside and sulfatide. Journal of Neurocytology 1998c;27:649–659. [PubMed: 10447239]

Dupree JL, Girault J-A, Popko B. Axo—glial interactions regulate the localization of axonal paranodal proteins. Journal of Cell Biology 1999;147:1145–1151. [PubMed: 10601330]

Ellisman MH, Levinson SR. Immunocytochemical localization of sodium channel distributions in the excitable membranes of Electrophorus electricus. Proceedings of the National Academy of Science of the U.S.A 1982;79:6707–6711.

Ellisman MH. Molecular specializations of the axon membrane at nodes of Ranvier are not dependent upon myelination. Journal of Neurocytology 1979;8:719–735. [PubMed: 541690]

Gilson JM, Blakemore WF. Schwann cell remyelination is not replaced by oligodendrocyte remyelination following ethidium bromide induced demyelination. Neuroreport 2002;13:1205–1208. [PubMed: 12151770]

Hille, B.; Catterall, W. Electrical excitability and ion channels. In: Siegel, GJ.; Agranoff, BW.; Albers, RW.; Molinoff, PB., editors. Basic Neurochemistry. 5th. Raven Press; 1994. p. 75-95.

Hiremath MM, Saito Y, Knapp GW, Ting JP-Y, Suzuki K, Matsushima GK. Microglial/macrophage accumulation during cuprizone-induced demyelination in C57Bl/6 mice. Journal of Neuroimmunology 1998;92:38–49. [PubMed: 9916878]

Honke K, Hirahara Y, Dupree J, Suzuki K, Popko B, Fukushima K, et al. Paranodal junction formation and spermatogenesis require sulfoglycolipids. Proceedings of the National Academy of Sciences of the U.S.A 2002;99:4227–4232.

Ishibashi T, Dupree JL, Ikenaka K, Hirahara Y, Honke K, Peles E, et al. A myelin galactolipid, sulfatide, is essential for maintenance of ion channels on myelinated axon but not essential for initial cluster formation. Journal of Neuroscience 2002;22:6507–6514. [PubMed: 12151530]

Kaplan MR, Cho M-H, Ullian EM, Isom LL, Levinson SR, Barres BA. Differential control of clustering of the sodium channels Nav 1.2 and Nav 1.6 at developing CNS nodes of Ranvier. Neuron 2001;30:105–119. [PubMed: 11343648]

Kaplan MR, Meyer-Franke A, Lambert S, Bennett V, Duncan ID, Levinson SR, et al. Induction of sodium channel clustering by oligodendrocytes. Nature 1997;386:724–728. [PubMed: 9109490]

Marcus J, Dupree JL, Popko B. Effects of galactolipid elimination on oligodendrocyte development and myelination. Glia 2000;30:319–328. [PubMed: 10797612]

Marcus J, Dupree JL, Popko B. Myelin-associated glycoprotein and myelin galactolipids stabilize developing axo-glial interactions. Journal of Cell Biology 2002;156(3):567–577. [PubMed: 11827985]

Mason JL, Langaman C, Morell P, Suzuki K, Matsushima GK. Episodic demyelination and subsequent remyelination within the murine central nervous system: changes in axonal caliber. Neuropathology and Applied Neurobiology 2001;27:50–58. [PubMed: 11299002]

Mason JL, Jones JJ, Taniike M, Morell P, Suzuki K, Matsushima GK. Mature oligodendrocyte apoptosis precedes IGF-1 production and oligodendrocyte progenitor accumulation and differentiation during demyelination/remyelination. Journal of Neuroscience Research 2000;61:251–262. [PubMed: 10900072]

Mathis C, Denisenko-Nehrbass N, Girault J-A, Borrelli E. Essential role of oligodendrocytes in the formation and maintenance of central nervous system nodal regions. Development 2001;128:4881–4890. [PubMed: 11731467]

Matsushima GK, Morell P. The neurotoxicant, cuprizone, as a model to study demyelination and remyelination in the central nervous system. Brain Pathology 2001;11:107–116. [PubMed: 11145196]

McMahon EJ, Cook DN, Suzuki K, Matsushima GK. Absence of macrophage-inflammatory protein-1alpha delays central nervous system demyelination in the presence of an intact blood-brain barrier. Journal Immunology 2001;167:2964–2971.

Rasband MN, Taylor CM, Bansal R. Paranodal transverse bands are required for maintenance but not initiation of Nav1.6 sodium channel clustering in CNS optic nerve axons. Glia 2003a;44:173–182. [PubMed: 14515333]

Rasband MN, Kagawa T, Park EW, Ikenaka K, Trimmer JS. Dysregulation of axonal sodium channel isoforms after adult-onset chronic demyelination. Journal of Neuroscience Research 2003b;73:465–470. [PubMed: 12898531]

Rios JC, Rubin M, St Martin M, Downey RT, Einheber S, Rosenbluth J, et al. Paranodal interactions regulate expression of channel subtypes and provide a diffusion barrier for the node of Ranvier. Journal of Neuroscience 2003;23:7001–7011. [PubMed: 12904461]

Rosenbluth J. Central myelin in the mouse mutant shiverer. Comparative Neurology 1980;194:639–648.

Rosenbluth J, Dupree JL, Popko B. Nodal sodium channel domain integrity depends on the conformation of the paranodal junction, not on the presence of transverse bands. Glia 2003;41:318–325. [PubMed: 12528185]

Smith MR, Smith RD, Plummer NW, Meisler MH, Goldin AL. Functional analysis of the mouse Scn8a sodium channel. Journal of Neuroscience 1998;18:6093–6102. [PubMed: 9698304]

Tompkins SM, Fuller KG, Miller SD. Theiler's virus-mediated autoimmunity: local presentation of CNS antigens and epitope spreading. Annals of the New York Academy of Sciences 2002;958:26–38. [PubMed: 12021081]

Traka M, Dupree JL, Popko B, Karagogeos D. The neuronal adhesion protein TAG-1 is expressed by Schwann cells and oligodendrocytes and is localized to the juxtaparanodal region of myelinated fibers. Journal of Neuroscience 2002;22:3016–3024. [PubMed: 11943804]

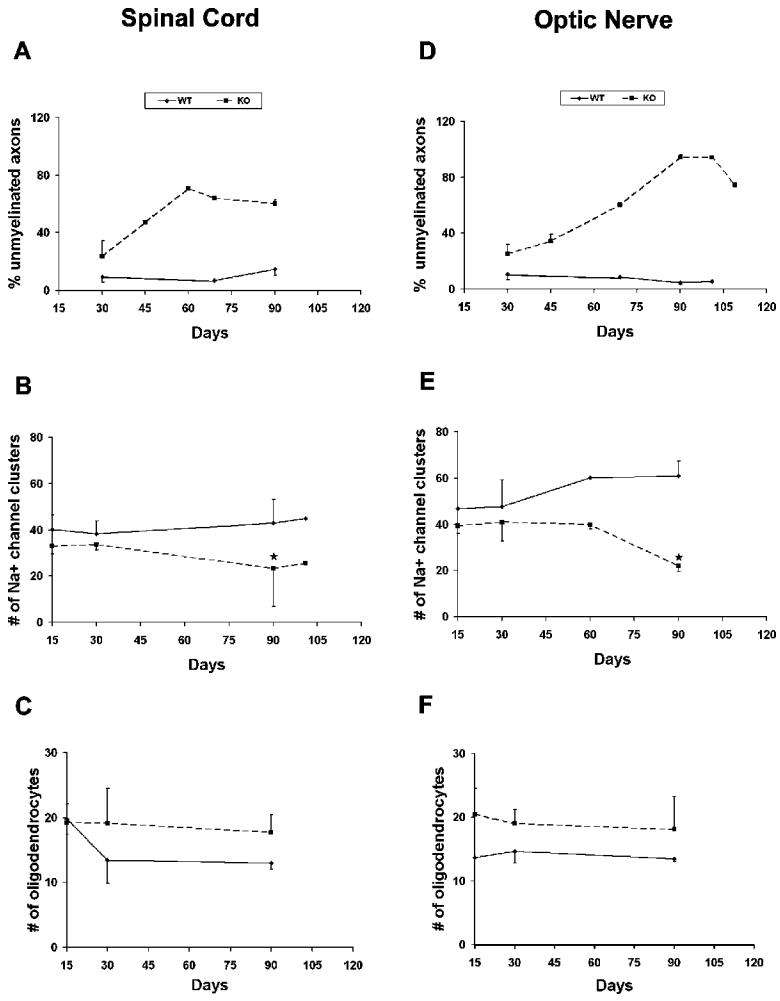


**Fig. 1.**

**Extensive spontaneous adult-onset demyelination in the CNS of CGT-mutant mice**. In the spinal cord (A) and optic nerve (D) of mutant animals, ~25% of axons are unmyelinated at 30 days. Because no signs of demyelination are present at this age, it appears that a many CNS axons in this mutant are never myelinated. By 45-days old, the number of unmyelinated axons increases in both CNS regions, which indicates the onset of demyelination. In the spinal cord, unmyelinated axons are most prevalent at 60 days old. At 69 and 90-days old, slightly fewer unmyelinated axons are observed, which indicates that remyelination outpaces demyelination. In the optic nerve, demyelination is more complete, with ~95% of axons lacking myelin by 90 days of age. By PND 109, the decrease in the number of myelin-bare axons and the presence of very thin myelin indicates that remyelination had begun. The relative number of $Na^+$ channel clusters (B,E) and oligodendrocytes (C,F) were also compared in the spinal cord and optic nerve of wildtype (WT) and CGT-knockout (KO) mice. At PNDs 15 and 30 the reduction in the number of channel clusters was not statistically significant. By PND 90, the number of clusters was significantly lower in the CGT-mutant mice compared with age-matched WT and PND 30 mutant animals. Importantly, the number of $Na^+$ channel clusters in the optic nerve of CGT-mutant animals did not decrease between PNDs 30-60. The number of oligodendrocytes was greater in the mutant mice at all ages, but this was not statistically significant. Data are mean ± S.D. of the number of $Na^+$ channel clusters or oligodendrocytes per field. Each value was compiled from a minimum of six fields per mouse and the number of mice used for each data point is indicated. **P*<0.05, Student's *t*-test.

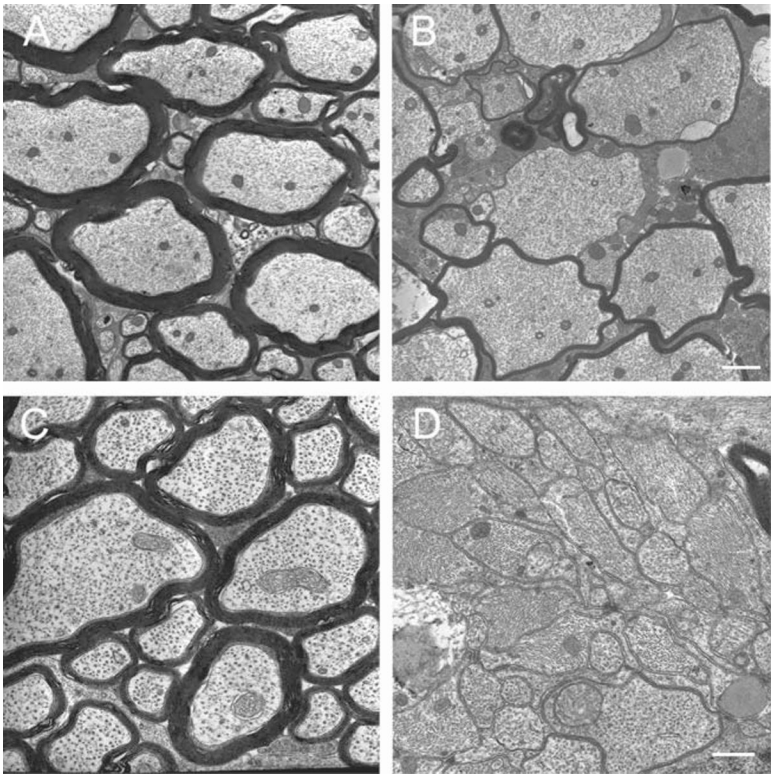


**Fig. 2.**

**CGT-mutant mice undergo extensive adult-onset demyelination**. Electron micrographs from spinal cord (A) and optic nerve (C) of 90-day-old WT mice. Demyelination is apparent in spinal cord (B) and optic nerve (D) of CGT-mutant mice. In the optic nerve, axons are devoid of myelin. In the spinal cord, many large axons lack myelin, but many axons have very thin myelin sheaths, which is indicative of remyelination. A,B; scale bar, 1 μm. C,D; scale bar, 0.5 μm.

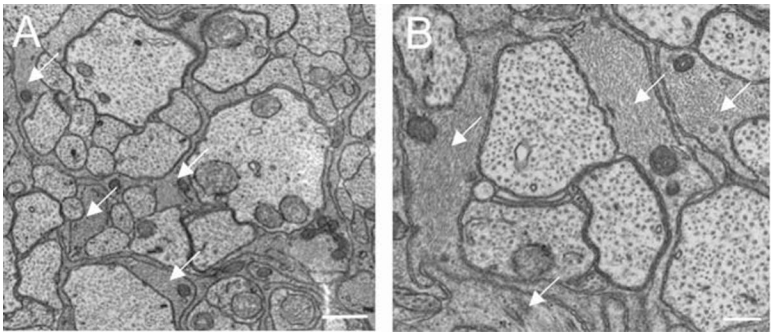


**Fig. 3.**

**Astrocytic processes are prevalent in the CNS of CGT-mutant mice**. (A) Electron micrograph from a 90-day-old CGT mutant shows that many unmyelinated axons are in contact with numerous glial processes (white arrows). (B) Higher magnification shows these glial processes to have astrocytic origin. A; scale bar, 500 nm. B; scale bar, 200 nm.

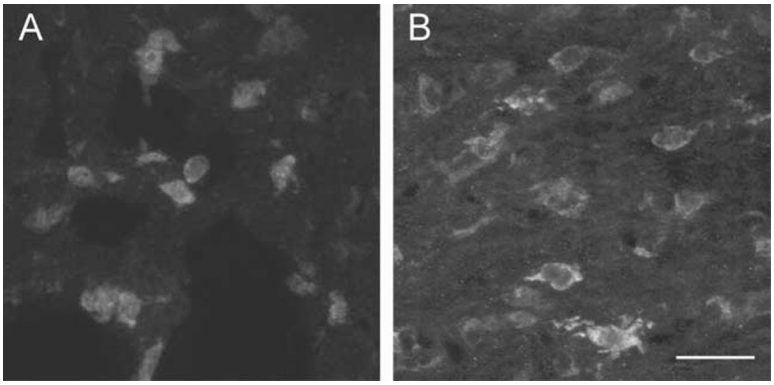


**Fig. 4.**

**The number of oligodendrocytes does not change in the CGT-mutant mice**. Longitudinal sections through the optic nerve of 90-day-old WT (A) and CGT-mutant mice (B) labeled with the cc-1 antibody, which is an effective marker of adult oligodendrocytes, shows that numerous oligodendrocytes are present. Scale bar, 5 μm.

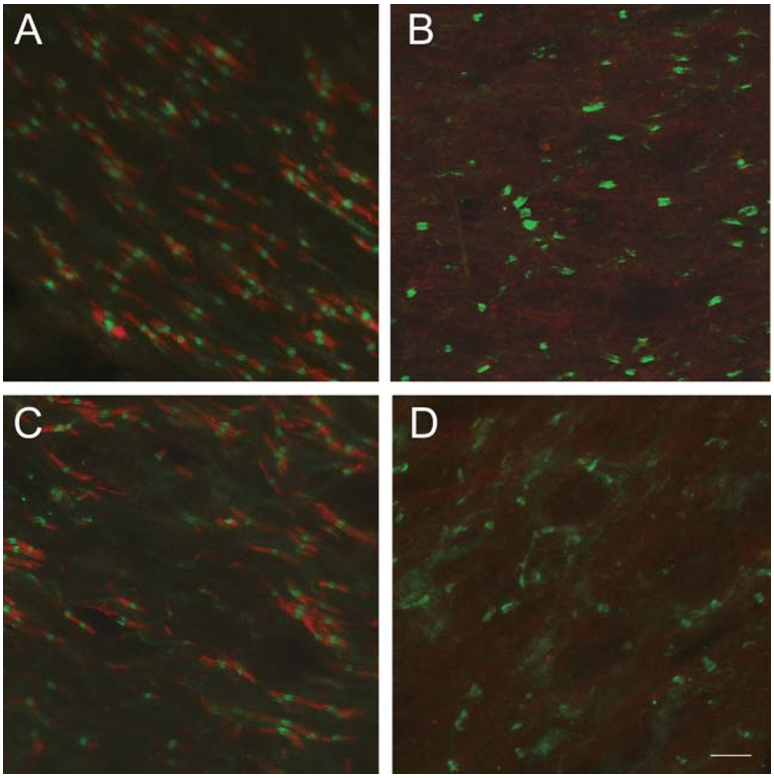


**Fig. 5.**

**The number of $Na^+$ channel clusters is not significantly reduced in CGT-mutant mice**. Unlike other demyelinating models in which oligodendrocyte death is prevalent, $Na^+$ channel clusters are partially preserved for several weeks after the initiation of demyelination. Cryosections of optic nerves from 30-day-old WT (A) and CGT-KO (B) mice immunoreacted against a pan-$Na^+$ channel antibody (green) and an antibody directed against the axolemmal protein NCP1 (red). Many $Na^+$ channel clusters are observed in both WT and mutant tissue. In the mutant tissue the clusters are slightly elongated but regular in shape. By contrast, $Na^+$ channel domains in a 90-day-old mutant (D) are less intense and frequently more irregularly shaped compared with a WT littermate (C). Scale bar, 5 μm.

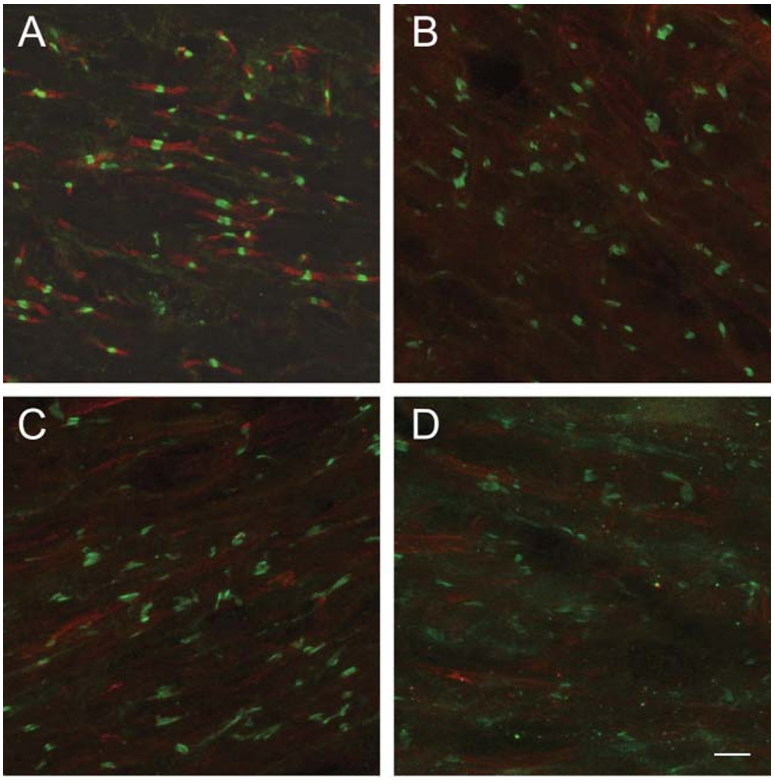


**Fig. 6.**

**A significant number of $Na^+$ channel clusters are present 8 weeks after the onset of spinal cord demyelination**. In the spinal cord of 30-day-old WT (A) and CGT-mutant (B) mice, numerous $Na^+$ channel clusters (green) are present. Similar to the optic nerve, $Na^+$ channel clusters in the spinal cords of CGT-mutants are slightly elongated and less regular in shape. At 90 (C) and 101 (D) days of age, $Na^+$ channel clusters are evident, but their borders are less well defined. Scale bar, 5 μm.

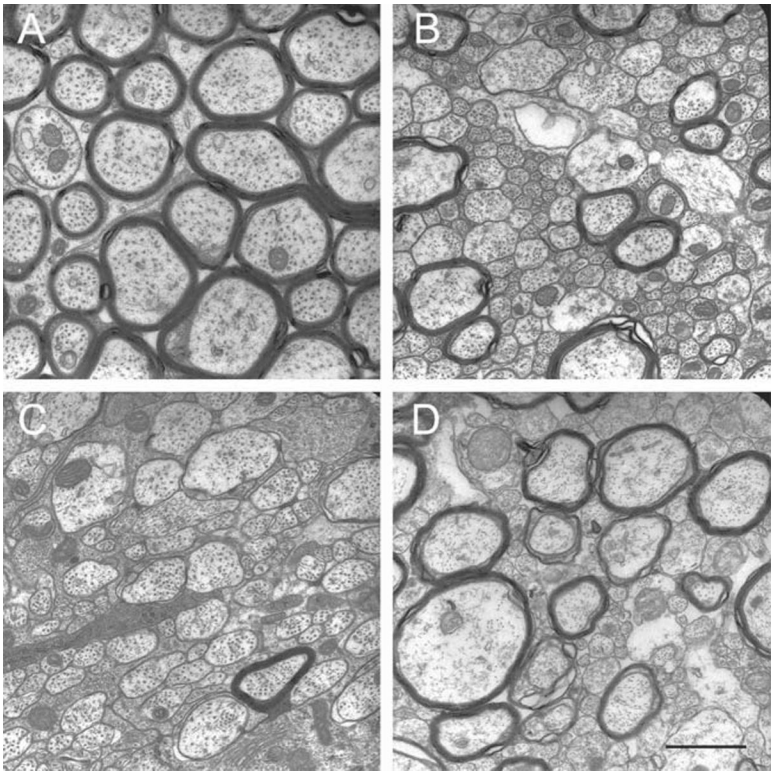


**Fig. 7.**

**The time course and extent of demyelination in the corpus callosum of adult mice treated with cuprizone**. (A) There is little evidence of demyelination after 2 weeks of treatment. Demyelination is extensive following 4 weeks of treatment (B) and almost no myelin is observed after 5 weeks (C). (D) Following 6 weeks of continuous treatment, many axons have thin myelin sheaths, which indicates remyelination. Scale bar, 1 μm.

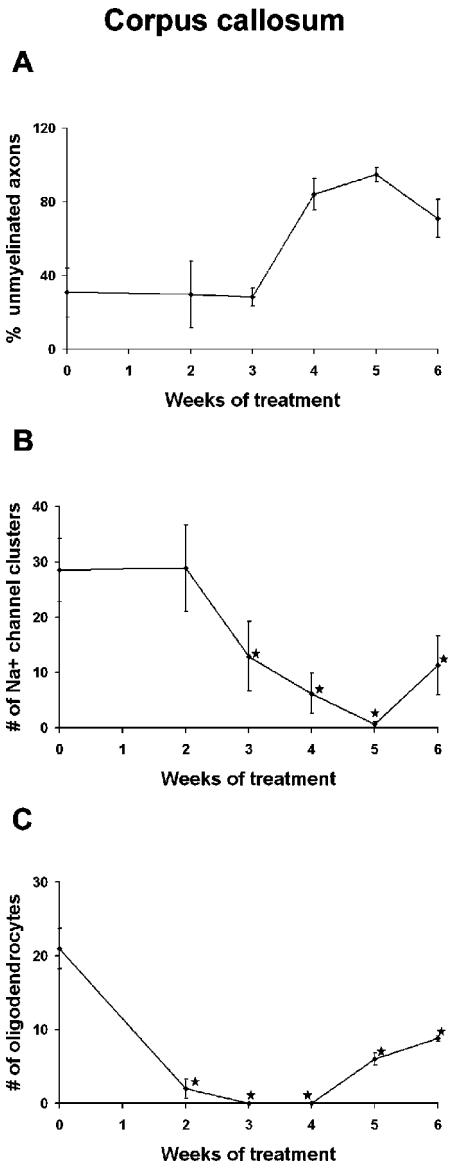


**Fig. 8.**

**Cuprizone induces extensive demyelination and reduces the numbers of $Na^+$ channel clusters and oligodendrocytes**. (A) Orally administered cuprizone induces extensive demyelination after 4 weeks of treatment. Corresponding to previous studies, remyelination was apparent by 6 weeks of continuous cuprizone treatment. (B) The relative number of $Na^+$ channel clusters was reduced significantly in mice treated with cuprizone for 3, 4, 5 and 6 weeks, whereas the number of oligodendrocytes was reduced significantly following 2 weeks of treatment (C). Thus, $Na^+$ channel clusters did not begin to disappear until after significant oligodendrocyte death. Values are mean ± S.D. of the number of $Na^+$ channel clusters and oligodendrocytes per field, with each value compiled from a minimum of six fields per mouse. *P<0.05, compared with mice maintained on a non-cuprizone containing diet (Student's *t*-test).

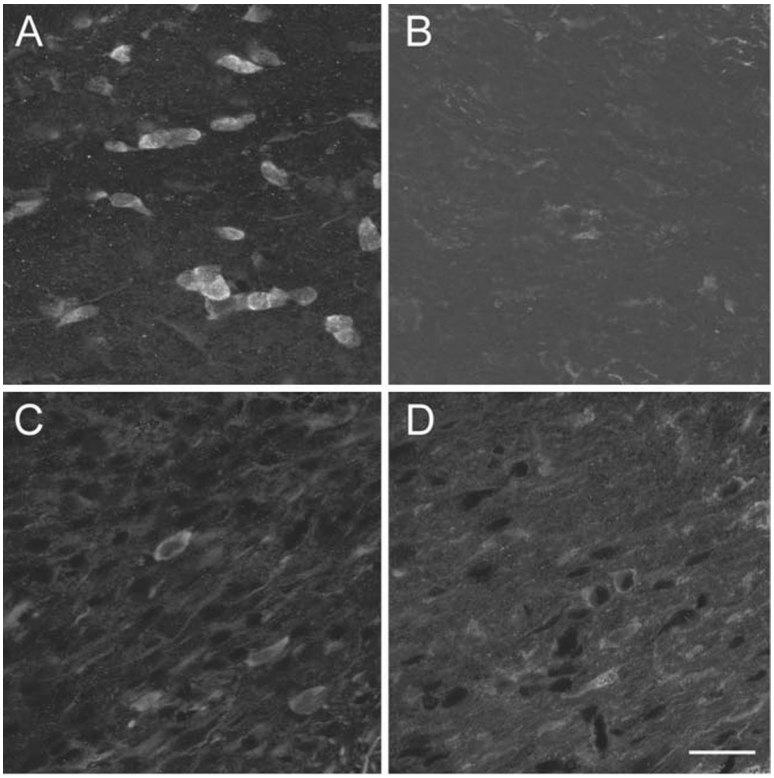


**Fig. 9.**

**Oligodendrocyte death is followed by the repopulation in the corpus callosum**. Frozen sections of the corpus callosum from untreated mice (A) and mice treated with cuprizone for 2 (B), 5 (C) and 6 (D) weeks show the chronological progression of oligodendrocyte death and repopulation. By 2 weeks of treatment, cc-1 immunolabeling shows the corpus callosum to be devoid of oligodendrocytes. Following 5 weeks of treatment, oligodendrocytes begin to migrate into the corpus callosum and repopulation continues throughout the remainder of the study. Scale bar, 10 μm.

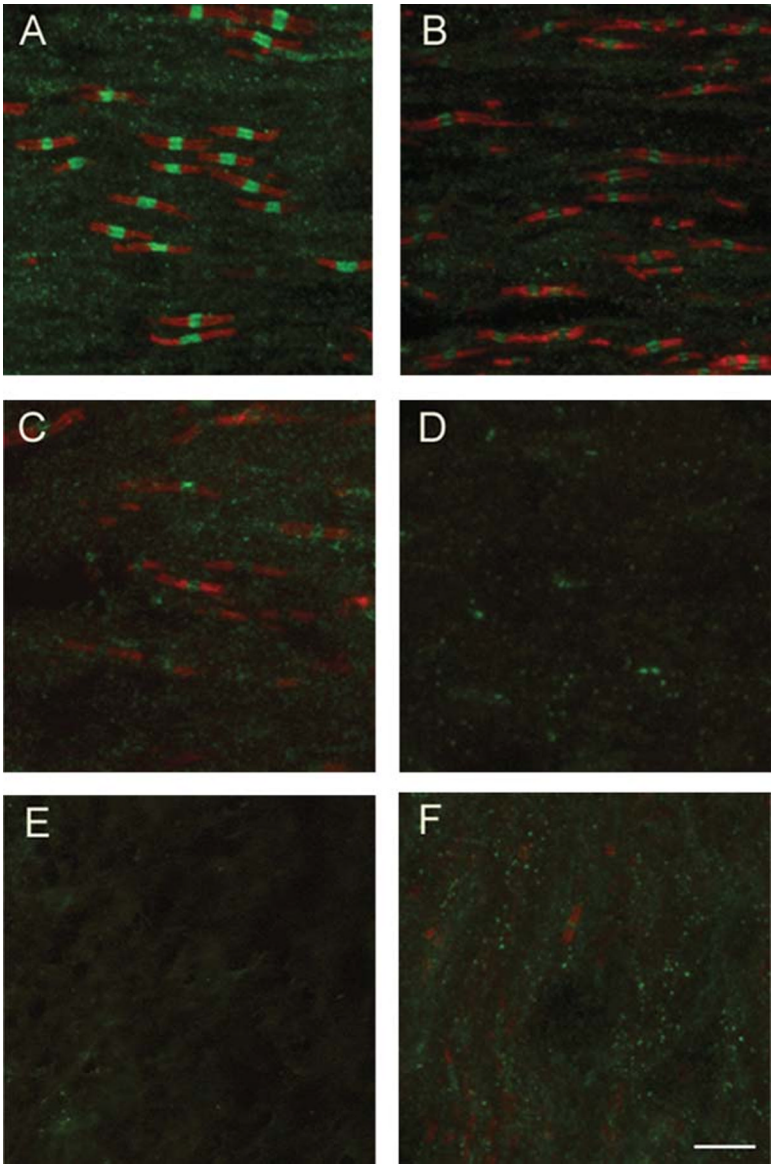


**Fig. 10.**

**Demyelination and oligodendrocyte death results in rapid loss of $Na^+$ channel clusters**. Double labeling for $Na^+$ channels (green) and NCP1 (red) in the corpus callosum of untreated mice (A) and mice fed cuprizone for 2 (B), 3 (C), 4 (D), 5 (E) and 6 (F) weeks shows that loss of $Na^+$ channel and NCP1 domains is evident following 3 weeks of treatment (C). Almost no $Na^+$ channel labeling is observed after 4 weeks of treatment. Demyelination starts between the 3rd and 4th weeks of treatment, with maximal loss of myelin at 5 weeks (see Fig. 9). Thus, $Na^+$ channel domains were lost within 2 weeks of the onset of demyelination in the absence of oligodendrocytes. Scale bar, 5 μm.

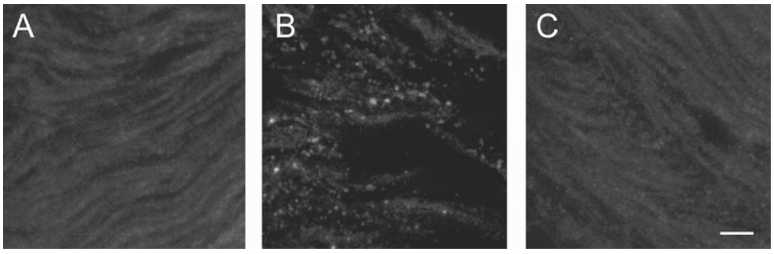


**Fig. 11.**

**Following demyelination, newly formed $Na^+$ channel clusters contain the immature $Na^+$ channel isoform**. (A) Immunoreactivity against $Na_v$ 1.2 is minimal in the corpus callosum of adult mice treated with cuprizone for 2 weeks. (B) $Na_v$ 1.2 labeling is present after 6 weeks of treatment, when there is evidence of substantial remyelination. The $Na_v$ 1.2 clusters are small, which is suggestive of immature clusters that give rise to the mature nodes of Ranvier. (C) $Na_v$ 1.2 reactivity is not present after 6 weeks of treatment with cuprizone followed by 2 weeks of normal diet to maximize remyelination. This indicates that $Na_v$ 1.2 expression is transient, which mimics its expression profile during development. Scale bar, 5 μm.